MAGNETOHYDRODYNAMICS Vol. 58 (2022), No. 4, pp. 483–490
DOI: 10.22364/mhd.58.4.12

STUDY OF HEAT TRANSFER IN A NICKEL DROPLET IN ELECTROMAGNETIC LEVITATION

R. Pons, A. Gagnoud, D. Chaussende, O. Budenkova

University Grenoble Alpes, CNRS, Grenoble INP, SIMAP, F-38000 Grenoble, France
e-Mail: romain.pons1@grenoble-inp.fr

Under terrestrial conditions, the temperature behaviour of a sample in levitation may be different from that observed in microgravity. Here we present the temporal evolution of the polar and equatorial temperatures of a levitating charge of Ni, revealed numerically and experimentally for different AC current modulations. It is demonstrated that the motion of the sample during the AC current modulation should be taken into account.

Introduction.

Electromagnetic levitation allows a metal sample, both in the solid and in the liquid state, to be held in space without any support due to the electromagnetic forces [1–3]. Coupling of this method with microgravity reduces the problem of levitation to the stabilization of a sample near an equilibrium point and provides multiple advantages because of the spatial symmetry of the system. Thus, a method of modulated calorimetry implemented in the Materials Space Laboratory at the International Space Station for the measurement of thermophysical properties of liquid metals is based on the so-called two-zone approximation [4, 5] that can be actually achieved only with the use of a symmetrical electromagnetic (EM) system. Furthermore, this model is based on a diffusive heat transport in the sample meaning that the convective flow generated by the electromagnetic force inside the sample is rather weak. Yet, under terrestrial conditions the EM force should compensate the weight of the sample. That implies that the eddy current in the lower part of the sample is stronger than in its upper part and the same is true for the Joule power. Furthermore, convective flow in the liquid sample under terrestrial conditions is more important than in microgravity because of a higher EM force. Finally, since the EM field is not completely symmetric, the sample may change its position if the intensity of the electric current circulating in the system varies. Because of these effects, the validity of the measurement procedure via modulated calorimetry realized with the Joule heating produced by the electromagnetic system for terrestrial experiments is under question. In the present work we studied the thermal behavior of the sample using different modulations of the electric current circulating in the inductor to check if the measurement procedure presented elsewhere can be realized [6].

1. Experiments.

In the experiments, the EM inductor is placed in a quartz chamber that provides a good visibility of the sample. The setup is equipped with two bichromatic pyrometers which follow temperature evolution in the polar and equatorial areas of the sample. A high speed video camera is used to register the sample image, and a Rogowski probe is used to register the electric current in the inductor circuit. Experiments are performed under argon to avoid the oxidation of the sample. A generator which aliments the inductor produces an AC current, whose frequency is equal to 151 kHz. One can control the power delivered by the generator, the latter adapts the delivered electric current and the potential according to the commanded power. Variation of the power produced by the generator leads to the modification of the power released in the sample, that in principle allows one to perform the procedure of modulated calorimetry. It is pertinent to remind that the sample receives only a small part of the power produced by the generator, that is defined by the electric conductivity and the size of the sample as well as by the geometry and electric conductivity of the inductor.

At the beginning of the experiment the sample is solid and have a spherical shape. Once the levitation is started, the sample is heated, melted, and attains a stationary temperature defined by the equilibrium between the Joule power released in the sample and the heat losses which occur mainly by radiation. After that the procedure of modulated calorimetry can be started.

1.1. Experiments with periodic modulation of the AC current. In the first experiment the sample of the radius $R = 3.53$ mm is heated up to the stationary temperature 1955 K with the AC current $I_{\mathrm{AC}} = 322$ A (hereafter the effective, RMS, value for the AC current is used). Then the AC current is modulated with the amplitude $\Delta I_{\mathrm{AC},1} = 2.5\% I_{\mathrm{AC}} \approx 8$ A and the period $T_{\mathrm{mod},1} = 2$ s, ($\omega_{\mathrm{mod},1} = 3.14$ rad/s). It is found that during the variation of the AC current both temperatures, equatorial and polar (T_{e} and T_{p}) increased and finally stabilized at higher, slightly different values, 1958 K and 1957 K, for T_{e} and T_{p}, respectively, as shown in Fig. 1*a*. That result is in contradiction with the theory, according to which, after the initial perturbation due to the modification of the heating power, the relaxation of both temperatures T_{e} and T_{p} back to the stationary value is expected [7]. The increase in temperature is due to the sample motion related to the variation of the EM force and is discussed below in Section 2. The noise presenting in the temperature data from the pyrometers does not allow one to recognize clearly the amplitude of the temperature modulations, and the phase difference between the responses of T_{e} and T_{p} cannot be clearly observed.

To diminish the sample oscillation related to the modulation of the AC current, in the second series of the experiment the amplitude of the AC current variation is twice less, $\Delta I_{\mathrm{AC},2} = 1.25\% I_{\mathrm{AC}} \approx 4$ A, while the period is twice larger, $T_{\mathrm{mod},2} = 4$ s, ($\omega_{\mathrm{mod},2} \approx 1.57$ rad/s). Two samples with the radii $R = 3.53$ mm and $R = 3.84$ mm are considered. It is found that during the AC current modulation, the average values of both temperatures for a smaller sample remained nearly constant, whereas for a larger sample the average values of both temperatures slightly decreased below the initial stationary temperature value 1951 K, as presented in Fig. 1*b*. As in the previous case, for a smaller sample the amplitude of the temperature variation due to the current modulation is comparable with the noise level. For a larger sample, the oscillatory character of the equatorial temperature with an amplitude nearly of 2 K can be recognized. It is seen as well that the equatorial temperature response is in counterphase to the modulation of the AC current.

In the third experiment, Fig. 1*c*, the amplitude of the modulation of the AC current is increased up to $\Delta I_{\mathrm{AC},3} \approx 6\% I_{\mathrm{AC}} = 20$ A to increase the amplitude of the temperature oscillations, and the period of modulation is also increased, $T_{\mathrm{mod},3} = 6$ s, ($\omega_{\mathrm{mod},3} = 1.05$ rad/s). The thermal behaviour of the two samples with the sizes indicated above is studied. As in the first experiment, the average values of T_{e} and T_{p} increased for both samples and stabilized at a new level. For the larger sample the increase of the average value of the equatorial temperature was 13 K and 11 K for the polar temperature. For a smaller sample the values of both temperatures are very close during the modulation of the AC current, the average temperature increase was about 8 K.

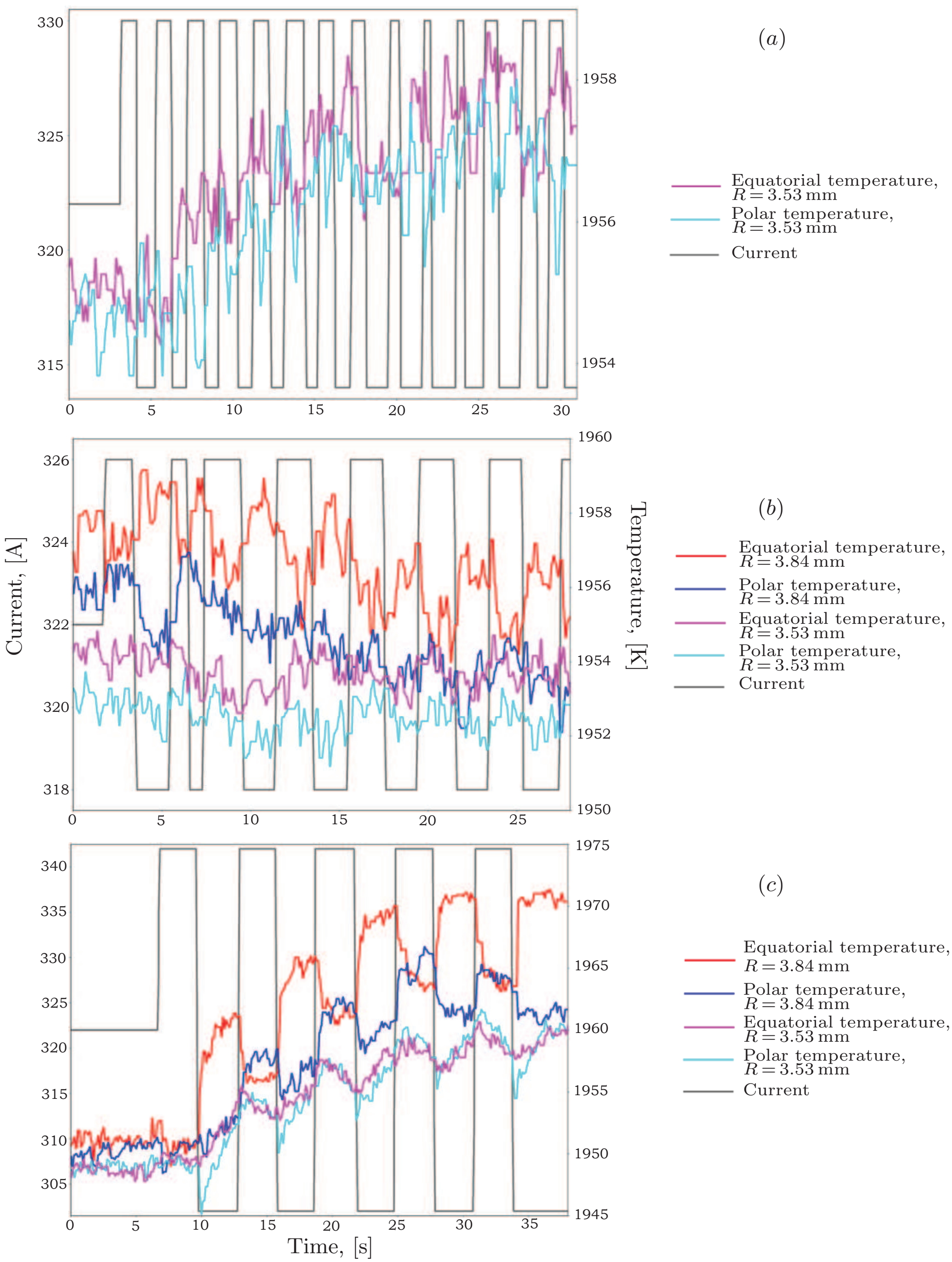

Fig. 1. Variation of equatorial and polar temperatures measured in the samples of different sizes during the periodic modulation of the AC current: for the sample $R=3.53$ mm (*a*) and $R=3.84$ mm (*b*,*c*): (*a*) $\Delta I_{\mathrm{AC},1}=8$ A, $T_{\mathrm{mod},1}=2$ s; (*b*) $\Delta I_{\mathrm{AC},2}=4$ A, $T_{\mathrm{mod},2}=4$ s; (*c*) $\Delta I_{\mathrm{AC},3}=20$ A, $T_{\mathrm{mod},3}=6$ s.

1.2. Discussion of experiments with periodic modulation of the AC current. According to theory [7], the total specific heat of the sample can be found via the amplitude of the power oscillations released in the charge ΔP_{mod} and the amplitude of the temperature response ΔT as follows

$$C_{\mathrm{p,tot}} = \frac{\Delta P_{\mathrm{mod}}}{\Delta T \cdot \omega_{\mathrm{mod}}} f(\omega_{\mathrm{mod}}, \dots). \tag{1}$$

The factor $f(\omega_{\mathrm{mod}}, \dots)$ in Eq. 1 takes into account the finite rate of the heat propagation through the sample and of radiative cooling, as well as the size of a zone of the sample which is heated directly.

Among the three experiments performed with the modulation of the AC current, only in the third one the amplitude of the temperature response can be clearly identified for the sample with the radius $R_{\mathrm{s}} = 3.84\,\mathrm{mm}$. For $\omega_{\mathrm{mod},3} \approx 1.047\,\mathrm{rad/s}$ and, provided that the rate of the internal heat propagation is much faster than the external cooling, which is valid for the case under consideration, $f(\omega_{\mathrm{mod}}, \dots) \approx 1$. The value of ΔP_{mod} can be estimated as follows. First, the Joule power released in the sample during the stationary stage prior to the current modulation, P_{st}, can be estimated via the heat balance (given by Eq. 2) provided the emissivity of the sample is known. That allows one to introduce a coupling coefficient α_{c} which relates the RMS value of the AC current circulating in the inductor and the power released in the sample. Then, this coefficient can be used to relate the measured amplitude of the AC current ΔI_{AC} to the ΔP_{mod}:

$$P_{\mathrm{st}} = 4\pi\varepsilon\sigma_{\mathrm{b}} R^2 (T_{\mathrm{st}}^4 - {T_{\mathrm{ext}}}^4) \tag{2}$$

$$\Delta P_{\mathrm{mod}} = \alpha_{\mathrm{c}} (I_{\mathrm{AC,max}}^2 - I_{\mathrm{AC,min}}^2) = \frac{2 P_{\mathrm{st}} \Delta I_{\mathrm{AC}}}{I_{\mathrm{AC,st}}} \tag{3}$$

where T_{st} is the temperature at the steady state measured by a bichromatic pyrometer, $I_{\mathrm{AC,st}}$ is the electric current at the steady state, $T_{\mathrm{ext}} = 300\,\mathrm{K}$ stand for the ambient temperature, and $\sigma_{\mathrm{b}} = 5.67 \cdot 10^{-8}\,\mathrm{W \cdot m^{-2} K^{-4}}$ is the Stefan–Boltzmann constant. Assuming the emissivity of Ni in the liquid state $\varepsilon = 0.33$, we obtain that the coupling coefficient for the sample $R = 3.84\,\mathrm{mm}$ during the stationary stage is $\alpha_{\mathrm{c}} = 4.83 \times 10^{-4}\Omega$, consequently, the amplitude of the power variation released in the sample is $\Delta P_{\mathrm{mod}} = 12.44\,\mathrm{W}$ and the total specific heat of the sample is $C_{\mathrm{p,tot}} = 1.48\,\mathrm{J/K}$ that gives the specific heat for Ni $C_{\mathrm{p}} \approx 790\,\mathrm{J/(K \cdot kg)}$ at a temperature near 1955 K. This value seems a bit far from the value known to be $\approx 650\,\mathrm{J/(K \cdot kg)}$ at the melting temperature [8], and this can be due to several reasons. The first is that the calculated coupling coefficient varies with the position of the sample, consequently, accepting it constant we induce some error in the calculation. Secondly, the frequency of the modulation is still too high, with respect to the favorable conditions of study: $0.1 < \omega_{\mathrm{mod}} < 1\,\mathrm{rad/s}$ [4], which would allow one to obtain a correction factor f even closer to unity, especially for the Biot number relative to Ni [7]. Finally, the specific heat increases with the temperature, therefore, a higher value of C_{p} can be indeed expected at 1955 K than at the melting state.

It should be noted that if convective heat transport is excluded, then using the phase shift of the temperature response and the defined value of the specific heat one can determined the value of the thermal conductivity as well.

1.3. Experiments with step wise modulation of the AC current. Another method to estimate the specific heat of the sample is to study the exponential temperature response to the instantaneous cooling (or heating) of the sample. The necessary condition

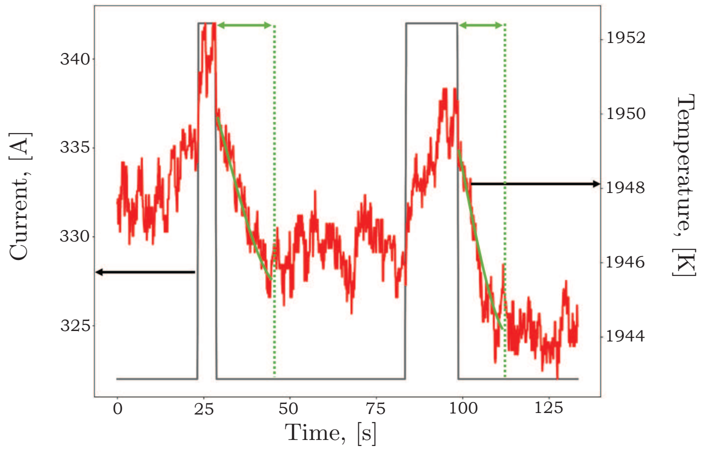

Fig. 2. Stepwise variation of the AC current (black), response of the equatorial temperature (red), and fitting curves (green), $R = 3.84$ mm.

Table 1. Results of C_p fitting for several samples.

	β	Residual, [K]	r^2	C_p, [J/(K·kg)]
$R = 3.84$ mm	0.0796	1.22	0.88	687
$R = 3.84$ mm	0.0797	0.99	0.91	684
$R = 3.78$ mm	0.0785	0.88	0.91	688

for this method to be valid, similar to the previous case, is that an inner heat transport in the sample is much more rapid than the external heat exchange. If this conditions fulfills, which is the case for the present work, then the temperature variations during the transition from one stationary state to another is of an exponential character:

$$\Delta T = B\mathrm{e}^{-\beta t} + D, \tag{4}$$

with $\beta = 4\pi R^2 \sigma_b \varepsilon T^3 / C_{p,tot}$, whereas the constants B and D correspond to two stationary temperatures. A stepwise heating procedure is applied for the two sample sizes $R = 3.84$ mm and $R = 3.78$ mm. An exampleof the data obtained for the sample with the radius $R = 3.84$ mm performed with different heating duration 5 s and 15 s is shown in Fig. 2. Then, the exponential fit using the Python function "*scipy.optimize.curve*" is applied to the measured variation of the equatorial temperature of each sample. Note that exponential fitting is very sensitive to the quality of the temperature scatter plot recovered by the pyrometer, and we did not apply any filters prior to the fitting.

The results obtained in the three experiments are summarized in Table 1, along with the maximum residual and the correlation coefficient between the fitting and the data (r^2). These results are closer to the value indicated elsewhere [8], the difference is due to the temperature value, at which the C_p is measured.

2. Numerical modelling.

The numerical modelling is performed with the COMSOL Multiphysics® (v5.6) software, details of the model, geometrical parameters and properties of the Ni sample are given elsewhere [9], except for C_p which is taken equal to 656 J/(K·kg) in this study [8]. The simulations were performed in the 2D axisymmetric geometry that well reproduces the global behaviour of the real system, except for the total power delivered to the

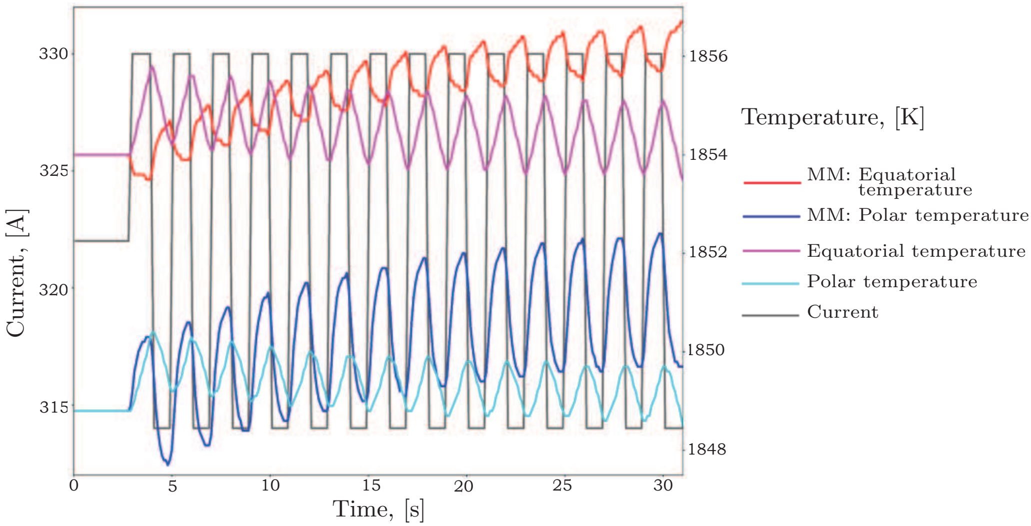

Fig. 3. Numerical calculations to evaluate the effect of sample motion, $\Delta I_{\mathrm{AC},1}$ $T_{\mathrm{mod},1}$, $R = 3.53$ mm, MM is for moving mesh.

system. The initial state in the modelling corresponds to the thermal equilibrium. It should be noted that the temperature in the sample is non-uniform if convective flow is not taken into account. The simulations were carried out in a transient mode, while the electromagnetic part was solved in the frequency domain. A time-dependent function was used to impose the variation of the RMS electric current in the coil. Convective flow in the sample is not taken into account. First, the modeling of heat transport during the AC current modulations was performed for a fixed position of the sample in the inductor. In the second modelling, the motion of the sample related to the variation of the AC current is considered with the use of the moving mesh (MM). Three different positions of the sample that correspond to the maximum, minimum and averaged value of the electric current were found from the experiment and used in the model.

The results of the modelling are illustrated in Fig. 3. For the stationary sample, the temperature variation follows the theory, i.e. after the initial perturbation, the average polar and equatorial temperature return to their stationary values. When the motion of the sample is taken into account, the average temperature increases, similar to the experimental observations shown in Fig. 1*a* and Fig. 1*c* because the average Joule power in the sample increases. Indeed, when the AC current decreases, the sample moves downward close to the coil and its coupling with the inductor increases, thus, the heating also increases and makes the equatorial temperature to increase as well, as shown in Fig. 1*c*. Comparison of the behavior of the polar temperature in modelling and in experiment is not representative, since the former does not consider account convective flow. In the experiment, the response of the polar temperature seems to be related to the size of the sample, which affects the sample displacement and the distance between the sample in its upper position and the upper inductor coil. Thus, a large sample can probably be heated from the top when the AC current has the maximum value that makes the polar temperature follow the variation of the AC current. For a smaller

Table 2. Results of C_p defined from numerical modelling.

	ΔP_mod [W]	ΔT, [K]	C_p, [J/(K·kg)]
Equatorial temperature	3.45	1.5	502
Polar temperature	3.45	1.1	685

sample, the polar temperature is defined by quite a rapid convective transport from the heated equatorial zone, and the behaviour of the polar and equatorial temperatures is similar.

The different values of C_p found numerically through Eq. (1) assuming that

$$f(\omega_\mathrm{mod}, \dots) = 1$$

are listed in Table 2. The C_p values are calculated only for a non-moving sample. Indeed, the case of moving sample is related to an imposed displacement and not to a displacement due to a change in electromagnetic forces.

The value of C_p closest to the one which is put in the model, is the one calculated with the variation of the polar temperature. In this case, the modelling corresponds to the purely diffusive heat transfer described by s two-zone model. The value is not exact because the modulation frequency used is not in the optimal range. This may explain why the best result is given by the ΔT of the pole and by the use of the 2D model which is limiting.

3. Conclusion.

The treatment of the experimental results issued from modulated electromagnetic calorimetry is based on the fact that the Joule power released in the sample totally correlates with the variation of the electric current circulating in the inductor and that the coupling coefficient between the load and the inductor is constant. However, in a non-symmetrical electromagnetic system the sample may move during the regular modulation of the AC current that makes the coupling coefficient variable and depending on the sample size, amplitude and frequency of modulation. Utilisation of larger samples allows one to decrease these displacements and also makes the difference between the polar and equatorial temperatures more remarkable. That makes the modulated calorimetry feasible under the terrestrial conditions.

4. Acknowledgments.

This work acknowledge the support from CNES for access to the data obtained in microgravity and used in simulations.

References

[1] D.M. Matson, *et al.* Use of thermophysical properties to select and control convection during rapid solidification of steel alloys using electromagnetic levitation on the space station. *Jom*, vol. 69 (2017), no. 8, pp. 1311–1318.

[2] M. Adachi, *et al.* Composition dependence of normal spectral emissivity of liquid Ni–Al alloys. *Isij International*, (2020), pp. ISIJINT–2020.

[3] M. Mohr, D.C. Hofmann, and H.-J. Fecht. Thermophysical properties of an fe57.75ni19.25mo10c5b8 glass-forming alloy measured in microgravity. *Advanced Engineering Materials*, vol. 23 (2021), no. 3, p. 2001143.

[4] H.-J. Fecht and W. Johnson. A conceptual approach for noncontact calorimetry in space. *Review of Scientific Instruments*, vol. 62 (1991), no. 5, pp. 1299–1303.

[5] J. Etay, *et al.* Measuring thermal conductivity and heat capacity of molten metallic alloys by electromagnetic levitation in DC field. *Magnetohydrodynamics*, vol. 53 (2017), no. 2; DOI: 10.22364/mhd.53.2.8

[6] P. Schetelat and J. Etay. A new approach for non-contact calorimetry: system identification using pseudo-white noise perturbation. *Heat and Mass Transfer*, vol. 47 (2011), no. 7, pp. 759–769.

[7] R.K. Wunderlich and H.-J. Fecht. Modulated electromagnetic induction calorimetry of reactive metallic liquids. *Measurement Science and Technology*, vol. 16 (2005), no. 2, p. 402.

[8] T.W. Chapman. The heat capacity of liquid metals. *Materials Science and Engineering*, vol. 1 (1966), no. 1, pp. 65–69.

[9] R. Pons, A. Gagnoud, D. Chaussende, O. Budenkova. Design of a coil for electromagnetic levitation: comparison of numerical models and coil realization. *Magnetohydrodynamics*, vol. 58 (2022), no. 1/2, pp. 55–64; DOI: 10.22364/mhd.58.1-2.6

Received 05.12.2022